

***Ab initio* investigation of noncontact atomic force microscopy tip-surface instability in InAs(110) surface**

V. Caciuc*

Fachbereich Physik, Universität Osnabrück, D-49069 Osnabrück, Germany and Institut für Festkörperforschung, Forschungszentrum Jülich, D-52425 Jülich, Germany

H. Hölscher

Center for NanoTechnology (CeNTech) and Physikalisches Institut, Westfälische Wilhelms Universität Münster, Wilhelm-Klemm-Str. 10, D-48149 Münster, Germany

S. Blügel

Institut für Festkörperforschung, Forschungszentrum Jülich, D-52425 Jülich, Germany

(Received 6 October 2004; revised manuscript received 16 February 2005; published 8 July 2005)

In the present work we report *ab initio* pseudopotential calculations based on density functional theory to investigate the noncontact atomic force microscopy (NC-AFM) image contrast on the InAs(110) (1×1) surface. The foremost tip structure is modeled by a SiH_3 tip. The effect of the tip-induced surface relaxations on the calculated forces was investigated for the tip above As and In atoms. The force curves corresponding to these vertical scans show an hysteretic behavior and this effect causes an energy dissipation of 0.3 (tip on top of As) and 1.8 eV (tip on top of In), respectively. The presence of this hysteresis suggests that stable NC-AFM images can be obtained for tip-sample distances before this instability. In this stable regime the force curves obtained for perturbed (due to tip-sample interaction) and unperturbed InAs(110) surface exhibit the same qualitative behavior. From the calculated forces for the unperturbed InAs(110) surface on a large number of grid points in real space we obtained maps of constant frequency shifts. The influence of long-range van der Waals forces on the simulated AFM images due to the macroscopic part of the tip was taken into account by an empirical model. The overall structure and the corrugation of the simulated NC-AFM images are in good agreement with the experimental results and allow us to explain the experimentally observed features of the image contrast mechanism on the basis of the calculated short-range chemical tip-sample interaction forces.

DOI: [10.1103/PhysRevB.72.035423](https://doi.org/10.1103/PhysRevB.72.035423)

PACS number(s): 68.37.Ps

I. INTRODUCTION

InAs is a well-investigated and well-understood direct-gap III-V semiconductor with a high carrier mobility which has already been used in a large variety of electronic and optic devices. A promising perspective with a potential significant technological impact is the use of this material in nanodevices which take advantage of the low dimensionality of the systems under consideration.^{1–5} For instance, quantum dots made of InAs are very attractive for quantum dot lasers, optical memory devices or high-speed electronics.^{6–8} From a technological point of view, the development of nanodevices requires a detailed knowledge of the surface structure at *atomic* scale because for such systems the surface effects may become at least as important as the bulk ones.

Exactly, the atomic surface structure of InAs was recently examined by Schwarz *et al.*^{9–11} using *noncontact atomic force microscopy* (NC-AFM).^{12,13} This microscopy technique is an extension of the *atomic force microscope* (AFM) (Ref. 14) which emerged as a very powerful experimental tool for surface scientists to image in real space the surfaces of conductors, semiconductors, and insulators. Originally, most atomic force microscopes operated in *contact* mode where tip and sample are in direct mechanical contact. Consequently, the obtained constant force maps were interpreted as the topography of the scanned surfaces. Despite this simple

physical interpretation of its outcome, the contact mode AFM failed to deliver “true” atomic resolution of the investigated surfaces in the sense that it is not able to image point-like defects even if the periodicity of the atomic surface is resolved. The reason for this failure is the elastic and plastic deformation of tip and surface due to adhesive forces.

These drawbacks have been overpassed by noncontact atomic force microscopy. The basic features of this technique reside in a cantilever oscillating near the sample surface. The most frequent experimental setup is the so-called frequency-modulation (FM) technique introduced by Albrecht *et al.*¹⁵ With this approach the cantilever oscillates always with a constant amplitude A at its actual resonant frequency f [see Fig. 1(a)]. Due to the tip-sample interactions this resonant frequency changes with the actual distance of the cantilever to the sample surface. During imaging, the frequency shift $\Delta f = f - f_0$ with respect to the eigenfrequency f_0 is kept constant by a feedback loop. Using this experimental setup in ultrahigh vacuum (UHV) true atomic resolution images of several types of surfaces are routinely obtained (for an overview see Refs. 16–18).

However, despite its practical success, the image contrast mechanism in NC-AFM is still a matter of debate. The underlying reason consists in a strong nonlinear behavior of the tip-sample interaction force, which acts on the tip only during a part of the cycling period. An intuitive picture of the

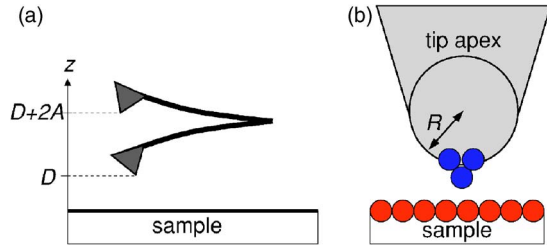


FIG. 1. (Color online) (a) Illustration of the experimental setup of a noncontact atomic force microscope. The cantilever with integrated tip vibrates with oscillation amplitude A close to the sample surface. The resonance frequency of the oscillating cantilever changes due to the interaction between tip and sample surface. (b) The tip-sample interaction is divided into short- and long-range forces. The long-range part is described by the van der Waals force between a spherical tip with radius R . The short-range forces between the foremost tip atoms and the surface are modeled by *ab initio* calculations where the tip is represented by a small atomic cluster.

physical origin of the atomic-scale resolution in NC-AFM can be reached from the analysis of the distance dependence of the various components of the total tip-surface interaction force. Since the long-range van der Waals or electrostatic forces do not vary significantly at the atomic scale, one can expect that the short-range chemical component of the tip-sample force is responsible for the atomic resolution in NC-AFM. This conclusion is supported by pioneering *ab initio* calculations performed by Pérez *et al.*^{19,20} (see also Ref. 21).

From a practical point of view, the problem to be solved in NC-AFM is to determine the correspondence between the positions of the atoms (defects) present on a given surface and the features (maxima and minima) of the recorded AFM image. As pointed out in literature (see, for instance, Ref. 22) this correspondence cannot be performed unambiguously only on the basis of structural (geometrical) considerations. An unambiguous assignment of the atomic positions in a NC-AFM image requires an accurate knowledge of the tip-sample interaction necessary in order to calculate the frequency shift.^{23,24}

These difficulties can be overcome by first-principle simulations providing a firm basis to interpret the observed features of the experimental NC-AFM images. To make possible such parameter-free calculations, the macroscopic tip is typically modeled by a microscopic tip attached to a macroscopic body [see Fig. 1(b)]. The microscopic tip which actually represents the apex structure of the experimental AFM tip is used in simulations in order to obtain the short-range chemical tip-sample forces which are thought to be responsible for the experimentally observed atomic resolution. The long-range forces of the macroscopic part of the tip are commonly modeled by an empirical model.

In this paper we report about our *ab initio* calculations performed in order to elucidate the mechanism of the NC-AFM image contrast formation for the InAs(110) (1×1) surface. To reach this aim we focused on the calculation of the short-range tip-sample interaction forces, which are reliably described by density functional theory and calculated by *ab initio* methods. To accurately simulate NC-AFM images for

this surface we computed the three dimensional (3D) field of the tip-surface force over a dense mesh in real space. The subsequent calculation of the frequency shift enables the simulation of NC-AFM images which are in a good agreement with the experimental findings of Schwarz *et al.*^{9–11}

II. CALCULATION SCHEME

Since the image contrast in noncontact atomic force microscopy is caused by the change of the resonance frequency of the oscillating cantilever, it is a prerequisite to recall the relationship between the tip-sample interaction and the shift of the resonance frequency. This issue has been analyzed by numerical²⁵ as well as analytical^{23,26,27} approaches. In many cases—especially for the results of Schwarz *et al.*^{9–11} obtained for InAs—the experimental oscillation amplitude is considerably larger than the tip-sample interaction range ($D \ll A$) and it can be shown that the relation between the tip-sample force F_{ts} and the frequency shift Δf is given by the integral equation^{23,26}

$$\Delta f(D, A) = \frac{1}{\sqrt{2\pi c_z A^{3/2}}} \int_D^\infty \frac{F_{ts}(z)}{\sqrt{z-D}} dz. \quad (1)$$

where c_z is the bending spring constant of the cantilever and D is the nearest tip-sample position [see Fig. 1(a)]. In UHV the tip-surface interaction force $F_{ts}(z)$ is given by the superposition of the short-range chemical forces F_{chem} and the long-range

van der Waals (F_{vdW}) and electrostatic (F_{electr}) ones. Since our simulations have been performed for zero applied bias voltage, only the effect of the long-range van der Waals forces on our NC-AFM results will be discussed in the following.

With this equation it is straightforward to calculate the frequency shift if the tip-sample force is known. In the case of van der Waals surfaces like xenon(111) (Refs. 24 and 28) and HOPG(0001) (Ref. 22) the interaction force can be obtained by a simple summation of pair potentials, but for semiconductors like InAs this procedure can lead to unreliable results. Therefore, we applied the following *ab initio* calculation scheme to determine the short-range chemical component of the tip-sample force generated by the microscopic tip and InAs(110) surface interaction.

Total energy calculations of the InAs(110) surface have been performed within the framework of density functional theory²⁹ in the local density approximation.³⁰ The Kohn-Sham equations have been solved self-consistently using the pseudopotential method³¹ as implemented in our fully parallelized EStCoMPP code.³² The full ionic potentials were replaced by smooth pseudopotentials using the same reference states as described in Ref. 33 while for H atom we used the bare Coulomb potential. The InAs(110) (1×1) surface was modeled by a slab consisting of five layers of In and As atoms separated by a vacuum region corresponding to eight atomic layers ($\approx 15.5 \text{ \AA}$). The corresponding supercell was constructed using the theoretical lattice parameter 6.041 \AA obtained for bulk InAs which is 0.3% smaller than the experimental value of 6.06 \AA .³⁴ In order to avoid the interac-

tion between the AFM tip and its periodically repeated replicas due to periodic boundary conditions we used a (2×2) surface unit cell. A fractional charged hydrogen layer has been employed to passivate the bottom surface as shown in Fig. 3(a). The positions of the atoms for three atomic layers counting from the bottom surface were fixed to their bulk values while those belonging to two surface layers were relaxed in the absence of the AFM tip.

Since the experimental NC-AFM images were recorded using silicon tips,^{9–11} for the microscopic part of the AFM tip we employed a SiH_3 molecule with three dangling bonds saturated by three H atoms and one dangling bond pointing towards the surface. This choice is similar to the AFM tip used by Sasaki *et al.*³⁵ and Ke *et al.*³⁶ From the physical point of view this option corresponds to a rather stiff tip, since we neglect the tip relaxation by this choice. This option has also been used by Huang *et al.*³⁷ in order to simulate the tip-sample interaction between silicon tips and the $\text{Si}(111)-(7 \times 7)$ surface. Larger tips might show relaxations or multi-bond interactions, if they are close to the surface. Another important issue is the tip morphology and its orientation relative to the sample surface. These effects have been extensively discussed in literature (see, for instance, Refs. 38–40). It is important to note that the interactions might depend on the tip morphology and its orientation. However, since the exact atomic structure of the tips is unknown in nearly all NC-AFM experiments, it is not *a priori* clear which tip structure is the best choice for a theoretical study. In this context, our tip-sample force curves might look different with other tips. Nonetheless, this observation is also true for any other *ab initio* simulation of NC-AFM experiments.

The surface relaxation as well as the electronic structure calculations performed to simulate NC-AFM images have been carried out using a basis set which includes all plane waves up to a cutoff energy E_{cut} of 9.0 Ry. With this choice, the relaxed positions obtained for surface atoms were found to be in a good agreement with the results already reported in literature (see, for instance, Refs. 33 and 41). More specifically, in the first surface layer the As atoms relax outwards and the In ones inwards leading to a surface buckling of about 0.76 Å. This surface relaxation is accompanied by a charge transfer from In to As ions leading to filled dangling bonds of As ions and empty dangling bonds of In ones. Special care has been given to the accuracy of the calculated tip-surface forces, because they represent the basic input in the simulations of the NC-AFM images. To obtain accurate tip-sample interaction forces, the Brillouin zone integrations have been carried out using a $2 \times 4 \times 4$ Monkhorst-Pack⁴² \mathbf{k} -mesh. We carefully checked this computational setup with respect to the thickness of the vacuum region, a larger (3×4) surface unit cell, the Brillouin zone sampling and the number of plane waves in the basis set controlled by the parameter E_{cut} to ensure a good convergence of the calculated forces. In particular, a 3×4 supercell was used to check the accuracy of the details of the dynamics of As and In atoms at atomic scale. All *first-principles* calculations carried out for this larger supercell (3×4) have been done using only the gamma point. We found an overall agreement for both supercells, and all presented data were obtained for the

2×2 supercell. A peculiar exception was the retraction force curve calculated for the tip on top of In atom. Since the tip tends to “pick up” the In atom from the surface during retraction, it was necessary to use the larger 3×4 supercell to get reliable results.

As already briefly discussed in the Introduction, the AFM tip is modeled by a microscopic and macroscopic part. One reason for this separation is that the current state-of-art exchange-correlation functionals used in the current *ab initio* methods do not describe properly the long-range van der Waals interaction. Besides this, the tip oscillation period is several orders of magnitude larger than that of the substrate’s phonons, and thus an *ab initio* simulation of the interaction of the *mesoscopic* tip with the surface is not possible due to finite computational time.

However, when simulating AFM images it is essential to take into account the long-range van der Waals forces acting between the macroscopic tip and the sample in order to obtain NC-AFM images at the experimental value of the frequency shift as well as the experimental corrugation.^{43,44} This is accomplished by adding to the *ab initio* calculated forces the long-range van der Waals forces due to the macroscopic part of the tip.⁴⁵ As other authors, we model this macroscopic part of the tip by a sphere with radius R [see Fig. 1(b)]. The corresponding long-range force is then given by²³

$$F_{\text{vdW}}(z) = -\frac{A_H R}{6z^2}. \quad (2)$$

where A_H represents the Hamaker constant. This empirical model neglects retardation effects, but describes the long-range forces occurring in atomic force microscopy between tip and sample for most practical cases (see, e.g., Refs. 17 and 18). Since we are not aware of a better value, we used 1.865×10^{-19} J (Si-Si interaction in air^{19,38}) for the Hamaker constant. The tip radius was assumed to be 100 Å (value given by the manufacturer⁴⁶). Nonetheless, the qualitative results are independent of the chosen values in a wide range as discussed below.

With this procedure we calculated the tip-sample forces along a direction perpendicular to the sample surface. Then we determined the corresponding frequency shift curves using the integral equation Eq. (1). However, since $\Delta f \propto f_0/(c_z A^{3/2})$, it is advantageous to use reduced units. The *normalized frequency shift*²³

$$\gamma(D) := \Delta f(D, A) \frac{c_z A^{3/2}}{f_0} \quad (3)$$

is independent of the actual experimental values of A , c_z , and f_0 . Therefore, we use this definition throughout this paper. In this way the presented theoretical results are easier to compare with experimental data.

The behavior of the feedback in the experimental setup is modeled in the following way: After choosing a suitable normalized frequency shift γ_{const} we determined the corresponding nearest distance D at different scan positions (x, y) , i.e.,

we solved numerically the equation $\gamma(D) = \gamma_{\text{const}}$. This procedure results in maps and line scans of constant frequency shift similar to the experiment.

III. SIMULATION RESULTS

A. Tip-sample interaction forces at specific sites

One intrinsic difficulty in NC-AFM is represented by the fact that during the experiments the distance between the cantilever and the sample surface is not known. This situation raises the question of what is the relevance of the surface relaxation induced by the tip-sample interaction on the experimental output. The importance of this perturbation for systems such as Si, InP, and GaAs was discussed in literature^{38–40,47,48} by means of *ab initio* simulations. To get an insight concerning the relevance of this issue for InAs(110) surface, we analyzed the tip-induced surface relaxations when the tip oscillates above As and In atoms. The vertical tip oscillation was simulated by moving the SiH₃ tip in a direction perpendicular to the surface. The tip-sample distance z used to plot the theoretical force curves (or displacement curves) corresponding to these vertical scans is the vertical distance between the Si apex atom of the AFM tip and the surface terminating As atoms in their equilibrium ground state structure (see Refs. 47 and 48 for more details). In order to distinguish between the force curves obtained when the sample surface was relaxed from those calculated where the surface was not relaxed, we refer to perturbed and unperturbed calculations in the following. [The relaxation of the InAs(110) surface in the absence of the tip is considered in any case.]

In Figs. 2(a) and 2(b) we present the force curves as a function of the tip-sample distance z calculated for the SiH₃ tip on top of As and In atoms, respectively. The InAs(110) surface was allowed to relax due to tip-sample interaction for these calculations. A basic feature of these displacement curves is the presence of discontinuities induced by the jump of the As and In atoms at approximately 3.7 Å and 3.2 Å, respectively, along the surface normal direction when the tip moves towards the surface. The corresponding jump height is approximately 0.7 Å for both atoms. The physical origin of these jumps towards the tip consists in the formation at these distances of a chemical bond between the apex Si atom and the As and In ones. Besides this, the calculated force curve exhibits an additional local minimum for As atom at approximately 2.4 Å (in the repulsive region) related to the jump of one In atom from its nearest neighbor site in the normal direction with approximately 0.7 Å. A qualitative illustration of this behavior for As atom using a ball-and-stick model is presented in Figs. 3(b) and 3(c).

Moreover, for *both* atoms the theoretical displacement curves exhibit a hysteric behavior associated with the presence of two local energy minima for As and In atoms in a direction perpendicular to surface (see, for instance, Ref. 17, p. 291). In consequence, when the tip moves away from the surface, the As atom jumps back to the surface at approximately 3.9 Å with a normal displacement of approximately 1.0 Å. We evaluated the energy dissipation corresponding to this hysteric behavior of the calculated tip-sample interac-

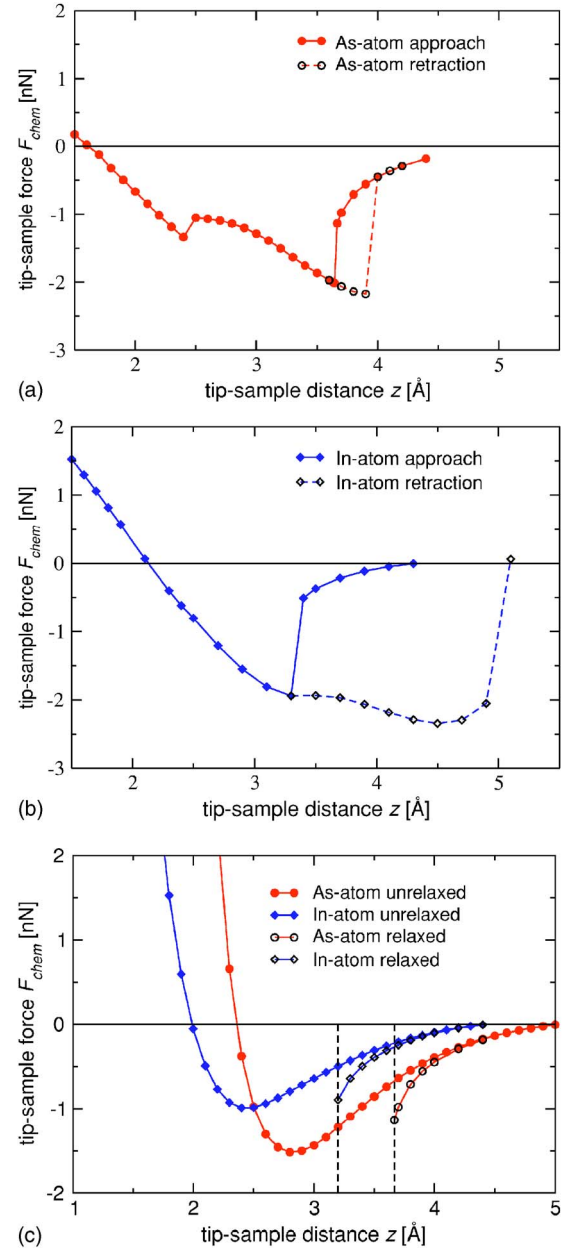


FIG. 2. (Color online) (a) The short-range tip-surface interaction force F_{chem} obtained for relaxed (due to tip-surface interaction) surface as a function of tip-sample distance z with respect to the position of the surface terminating As atom is shown for the SiH₃ tip on top of an As atom by symbols. (b) The same as in (a) on top of an In atom. (c) The calculated force curves obtained for relaxed and unrelaxed InAs(110) surface when the tip is above As and In atoms are shown by symbols. For the relaxed case, only the tip-surface forces calculated before the jumps of As and In atoms towards the tip are shown.

tion force to approximately 0.25 eV. In the case of the tip above the In atom, the retraction force curve exhibits a much larger hysteresis than that for the As one. This leads to a higher value of the energy dissipation (approximately 2.1 eV) and to a higher tip-surface distance (approximately 4.9 Å) from where it jumps back to the surface. The details of the atomic dynamics when SiH₃ tip is on top of the In site

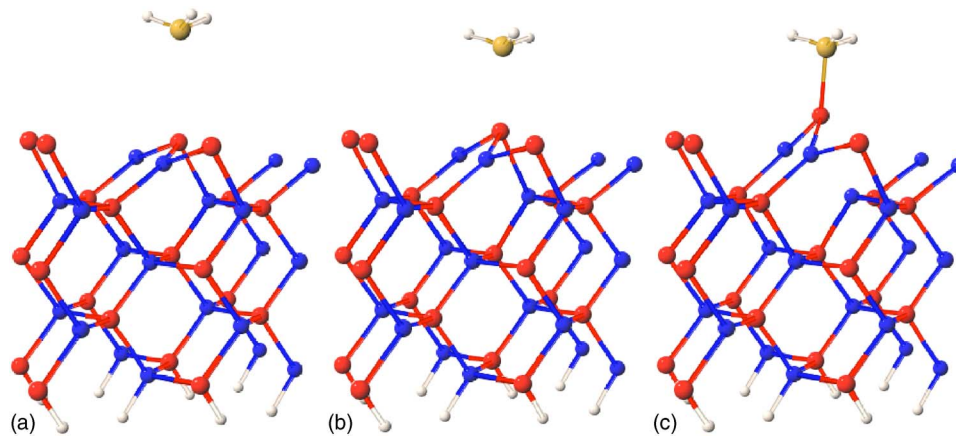


FIG. 3. (Color online) Ball-and-stick model for the relaxed supercell of InAs(110) (2×2) when the SiH_3 tip approaches the surface on top of an As atom. (a) For a tip-sample distance of ≈ 4.4 Å the InAs(110) is almost unperturbed by its interaction with the tip. (b) As the tip-surface distance is further reduced, the surface relaxation becomes significant. Here is a snapshot of the atomic structure for a tip-surface distance of ≈ 3.7 Å. (c) The jump of As atom at $z \approx 3.6$ Å due to the formation of a chemical bond between the Si apex atom and the As one is shown.

are reported in Fig. 4. Similar hysteretic behavior for Ga atom on GaAs(110) surface was reported by Ke *et al.*³⁹

In particular, for the tip on top of the In atom our *ab initio* simulations suggest that when the tip moves away from the surface it tends to pick up the In atom. This feature is displayed when the tip is at about 3.1 Å above the surface and is characterized by a normal displacement of In atom with a magnitude of approximately 2.3 Å with respect to its equilibrium position. For comparison, the similar displacement of As atom is about approximately 1.0 Å. This theoretical finding agrees well with the experimental observation that sometimes the AFM tip picks up atoms from sample surface which usually determines a dramatic change of the recorded NC-AFM images. For instance, the use of a clean Si tip leads to an invisible In sublattice in NC-AFM images while it becomes visible when using a tip which crashed into the InAs surface.^{9–11} However, a better insight into this rather delicate problem might be provided by the use of a larger tip in the simulations. Moreover, one should point out that in order to get reliable results for In dynamics when the tip

moves away from the surface a larger (3×4) supercell must be used in our calculations. The reason is that for a smaller in-plane surface unit cell one nearest neighbor As atom is trapped into an energy minimum due to a lack of relaxation freedom.

The presence of a hysteresis for both atoms has an important consequence for the stability of the NC-AFM operational mode on InAs(110) surface. More specifically, in order to ensure a *stable* feedback, our *ab initio* simulations suggest that the distance of closest approach D between tip and sample must range between approximately 3.7 Å (tip on top of As) and approximately 3.2 Å (tip on top of In) [see Fig. 2(b) for more details]. Since these distances are quite close to the upper limit of the range of the chemical forces (approximately 5 Å), the question is what is the relevance of the surface relaxation on the calculated interaction forces in this case.

In Fig. 2(c) we compare the displacement curves obtained for the SiH_3 tip on top of As and In atoms when the InAs(110) surface remains unperturbed by the tip-sample in-

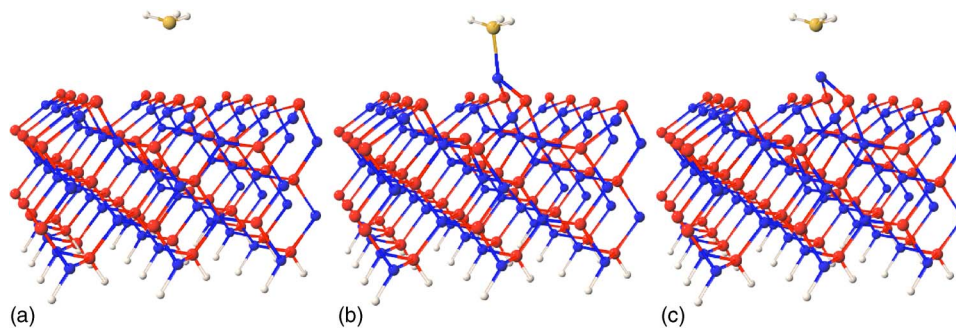


FIG. 4. (Color online) Ball-and-stick model for the relaxed supercell of InAs(110) (3×4) then the SiH_3 tip moves away from surface on top of an In atom. (a) As in the case of the tip on top of an As atom, when the tip moves towards the surface from large tip-sample distances (≈ 4.3 Å), the tip-sample interaction does not induce a significant relaxation of the InAs(110) surface. (b) At a tip-surface distance of ≈ 3.7 Å the In atom is pulled out from the surface due to its strong chemical interaction with the apex atom of the tip. The magnitude of the normal displacement of the In atom is ≈ 2.2 Å with respect to its equilibrium position. (c) At $z \approx 4.5$ Å the chemical bonding between In atom and Si one is broken and the In atom starts to return to its equilibrium position.

teraction with those obtained when the surface perturbation was included. In order to ease the comparison, for the case when the surface relaxation was taken into account only the data up to the atoms jump towards the surface are shown. One can observe a stronger interaction of the tip with the surface when it is on top of the As than when it is above the In atoms. This behavior is intrinsically related to the structure of the InAs(110) surface (in the absence of the tip). As mentioned before, to reach equilibrium in the first surface layer the As atoms relax outwards and the In ones inwards leading to a surface buckling of approximately 0.76 \AA . As a consequence of the charge transfer from In to As ions, the chemical interaction between the filled dangling bonds of As ions with that of the half-filled dangling bond of the Si apex atom is stronger than that between the empty dangling bonds of In with the dangling bond of the Si tip. One should mention that our results are similar to those reported in Ref. 39 for GaAs(110) surface.

By analyzing the above force curves one can observe that there are two additional effects of the surface relaxation besides the hysteresis, (i) in the repulsive region the magnitude of F_{chem} is significantly reduced when the surface relaxation is taken into account; (ii) there is a shift of the minimum of the calculated forces in the absence of surface relaxation to higher absolute values by approximately 0.7 nN and to smaller distances with respect to the InAs(110) surface. A key observation for our subsequent *ab initio* simulations is that in both cases (perturbed and unperturbed) the calculated force curves when the SiH_3 tip approaches the surface on top of the As atom are always on the “right” side (i.e., to higher tip-sample distances) with respect to those obtained for the In one. The direct consequence of this finding is that irrespective of the inclusion of the surface perturbation induced by the tip, the As atom will appear brighter in an NC-AFM image than the In one regardless of the magnitude of the long-range van der Waals forces. Moreover, as clearly shown in Fig. 2(c), for tip-surface distances at which a stable feedback can be maintained, the displacement curves calculated for perturbed and unperturbed cases show a quite similar shape although they differ in magnitude.

B. The simulation of a NC-AFM image

The results presented in the preceding section imply that for the SiH_3 tip the surface relaxation due to the tip-sample interaction does not *qualitatively* change the frequency shift maps obtained on the basis of short-range chemical forces. In consequence, we simulated NC-AFM maps of constant frequency shift by ignoring the surface relaxation due to its interaction with the tip. Of course, the calculation of the short-range forces including the additional relaxation of the sample surface due to the tip-sample interaction might provide a better agreement with the experiment but such *ab initio* calculations require too much computer time to get a complete NC-AFM image.

In order to simulate NC-AFM images for the InAs(110) surface, we calculated the normal component of the short-range chemical tip-sample forces $F_{\text{chem}}(x, y, z)$ at 32 (x_i, y_j) in-plane grid points regularly distributed in the irreducible

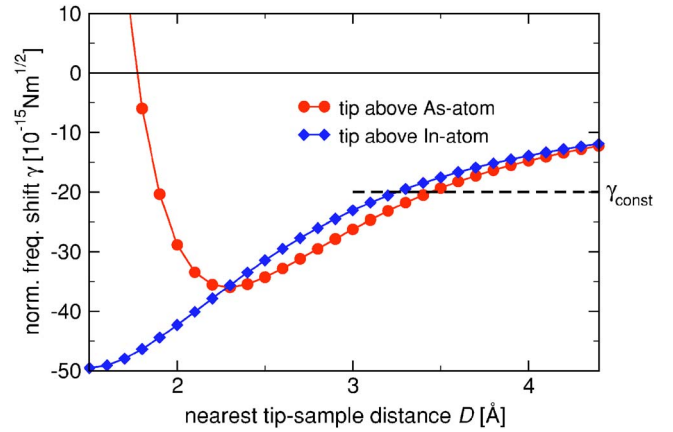


FIG. 5. (Color online) The normalized frequency shift is calculated taking into account the long-range van der Waals force. The NC-AFM image in Fig. 6 is obtained for a normalized frequency shift of $\gamma_{\text{const}} = -20 \times 10^{-15} \text{ Nm}^{-1/2}$.

wedge of the surface unit cell, which represents $1/8$ of the full $c(2 \times 2)$ surface unit cell. At each (x_i, y_j) point, the forces were calculated at 40 different z_n points perpendicular to the surface using an increment of 0.1 \AA . This amounted in total to about 1300 self-consistent calculations. In order to obtain an overall description of the tip-sample interaction force, we calculated the short-range interaction forces acting between the SiH_3 tip and InAs(110) surface for distances up to $z = 1.5 \text{ \AA}$ above the As atoms, even if in experiments such a short distance would imply a tip crash into the surface due to attractive tip-surface chemical bondings which may be formed at certain places on the surface. This huge amount of *ab initio* computations was necessary to obtain a good description of the interaction forces in real space without the need to fit our results to certain (possible inaccurate) model potentials. On this fine mesh the additional relaxation of the surface due to the tip-surface interaction was not included into the calculations.

Both the long-range *van der Waals* and the short-range *chemical* forces are considered for the calculation of the normalized frequency shift curves plotted in Fig. 5. The main feature displayed by these curves is a faster change of the normalized frequency shift with respect to the distance of closest approach D when the tip is above the As atom compared with the case when it is on top of the In one. This behavior suggests that the As site should be brighter than the In one. This assumption is confirmed by the detailed analysis of our simulated NC-AFM images.

In Fig. 6 we present a simulated NC-AFM image, which was calculated assuming a normalized frequency shift of $\gamma_{\text{const}} = -20 \text{ fNm}^{1/2}$. The basic feature of the simulated image is that only the As sublattice is imaged as it can be seen by a comparison with the surface structure of InAs(110) displayed on the right-hand side. Furthermore, it can be observed that the position of the In atom does not appear as a specific feature in the simulated NC-AFM image. The same result is obtained for other values of γ_{const} . We also checked the influence of different values of the Hamaker constant and/or the tip radius [see Eq. (2)]. By changing this value one can increase and decrease the corrugation of the simu-

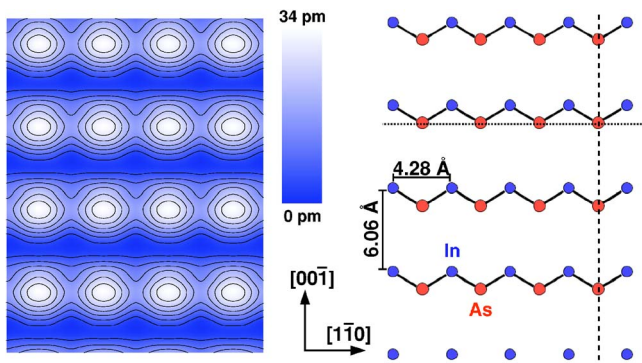


FIG. 6. (Color online) Simulated NC-AFM image for the relaxed InAs(110) surface structure. The surface structure is shown on the right-hand side for comparison. Notice that the As and In atoms are not in the same surface plane. The image size corresponds to the 4×4 unit cell. The dashed and dotted line mark the scan direction along the $[00\bar{1}]$ and $[1\bar{1}0]$ direction, respectively.

lated NC-AFM images, but the As sublattice is imaged in every case. The consideration of suitable offsets between the macroscopic and microscopic tip⁴⁹ does not change this result. In addition, we tried different tip geometries. However, the simulated NC-AFM images obtained for a cone and cone-sphere tips showed that—regardless of their geometrical parameters—only the As atoms are imaged as bright protrusions.

The emerging conclusion of this analysis is that the NC-AFM image contrast formation for the InAs(110) surface is mainly governed by short-range chemical forces, since the image contrast is independent of the assumed shape of the macroscopic tip. Similar results have been reported for other systems.^{19,40,47,48}

Finally, our simulated images are in agreement with the experimental ones obtained by Schwarz *et al.*^{9,10} Their analysis revealed that when using clean silicon tips the recorded NC-AFM images consisted of rows of bright protrusions which were assigned to the As atoms on the basis of a pure geometrical analysis. This conclusion, however, is fully confirmed by our calculations. The overall structure of the theoretical NC-AFM images agrees with the experiment. The corrugation height of the images is also comparable with the experiment. This is shown in Fig. 7 for the same value of frequency shift used for the simulated image presented in Fig. 6. The heights along the $[00\bar{1}]$ and $[1\bar{1}0]$ directions are about 28 pm and 15 pm, respectively. The experimental values are in the same order of magnitude depending on the actual tip shape and the chosen frequency shift.^{9–11} The dependence of the corrugation on the scan direction has also been observed by Schwarz *et al.*⁵⁰

As already briefly discussed above, a geometrical assignment between a NC-AFM image and a surface structure at atomic level might be misleading in some cases. The origin of this situation is that the tip-sample interaction forces depend on the charge density surrounding the atoms and usually there is no one-to-one correspondence between the topology of the electron density and the underlying atomic structure. This situation is in particular illustrated by the above-mentioned experimental work, where for tips which

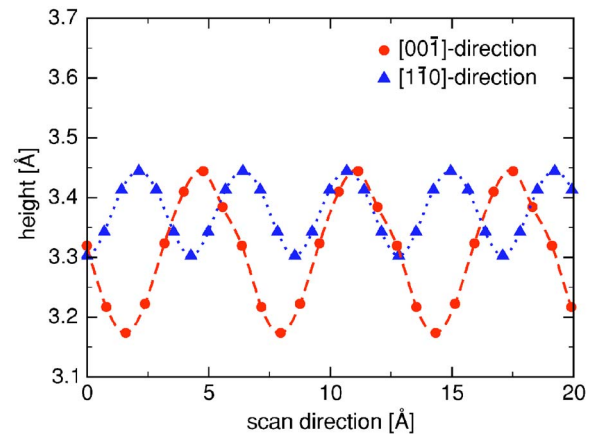


FIG. 7. (Color online) Calculated scan lines reveal a corrugation of ≈ 28 pm and ≈ 15 pm depending on the scan direction. The dashed and dotted line mark the scan lines along the $[00\bar{1}]$ and $[1\bar{1}0]$ directions, respectively. Both scan directions are marked in Fig. 6 by dashed and dotted lines, respectively.

previously crashed into the surface a second feature was imaged as minima or darker maxima (see Fig. 3 of Ref. 10) and it was assumed that it originates from In sublattice. This effect, however, could not be reproduced by the present work. From this difference between experiment and theory we conclude that our assumption that the tip apex consists of a single silicon atom with one dangling bond does not hold anymore for these tips. After an indentation of the tip into the sample surface the tip structure might be modified or the foremost tip atom might be changed to an In or As atom. In both cases the short-range chemical forces are modified resulting in a different NC-AFM image contrast.

IV. SUMMARY

By using the *ab initio* pseudopotential method, we have investigated the dynamics at atomic scale during the scanning process for a SiH_3 tip on top of As and In atoms on the InAs(110) surface. For vertical scans above these atoms the effects of tip-induced surface perturbation on the calculated tip-sample chemical forces have been investigated. Our *first-principles* simulations showed that the calculated force curves for *both* atoms show an hysteretic behavior associated with the jumps of these atoms. Due to the presence of this hysteresis, a stable operational mode of the NC-AFM for the InAs(110) surface is expected only at distances where these jumps do not occur.

In this stable regime, the force curves obtained with and without the consideration of the tip-sample interaction (perturbed and unperturbed case) show the same qualitative behavior and show no hysteresis before the discontinuity. Therefore, we assumed that the surface relaxation due to the tip-sample interaction does not *qualitatively* change the frequency shift maps obtained on the basis of short-range chemical forces. With this assumption, we simulated complete NC-AFM images for the InAs(110) surface for the unperturbed case. The short-range chemical tip-sample interaction forces as well as the long-range van der Waals force

were taken into account. In order to remove any inaccuracy of the calculated short-range chemical forces due to a fit to a potential model, we sampled the irreducible wedge of InAs(110) surface by a grid of ≈ 1300 points. We considered three different geometries for the macroscopic part of the AFM tip. Regardless of the geometry used, only the As atoms were imaged as maxima. This outcome does not change within a wide range of values for the Hamaker constant and the tip radius. Therefore, we conclude that the NC-AFM image contrast mechanism for InAs(110) surface relies on the short-range interaction between the half-filled dangling bond of the tip apex atom with that of As atoms. The long-range van der Waals force is relevant only for the corrugation of the experimental and theoretical NC-AFM images as well as

for the value of the constant frequency shift at which the theoretical NC-AFM images are simulated.

ACKNOWLEDGMENTS

The authors are indebted to A. Schwarz and F.-J. Giessibl for fruitful discussions concerning NC-AFM. Furthermore, the authors would like to mention continuous support from H. Fuchs and A. Schirmeisen. The computations were performed under the grant “Rasterkraftmikroskopie” on Cray computers of Forschungszentrum Jülich. This work was supported by the DFG (Grants Nos. BL 444/2-1 and HO 2237/2-1), the BMBF (Grant No.03N8704), and by the “Ministerium Wissenschaft und Forschung des Landes Nordrhein-Westfalen.”

*Present address: Physikalisches Institut, Westfälische Wilhelms Universität Münster, Wilhelm-Klemm-Str. 10, D-48149 Münster, Germany.

¹M. Johnson, B. R. Bennett, M. J. Yang, M. M. Miller, and B. V. Shanabrook, *Appl. Phys. Lett.* **71**, 974 (1997).

²D. Grundler, *Phys. Rev. B* **63**, 161307(R) (2001).

³M. B. Johnston, D. M. Whittaker, A. Corchia, A. G. Davies, and E. H. Linfield, *Phys. Rev. B* **65**, 165301 (2002).

⁴M. T. Björk, B. J. Ohlsson, C. Thelander, A. I. Persson, K. Depert, L. R. Wallenberg, and L. Samuelson, *Appl. Phys. Lett.* **81**, 4458 (2002).

⁵I. Vurgaftman and J. R. Meyer, *Appl. Phys. Lett.* **82**, 2296 (2003).

⁶E. Moreau, I. Robert, J. M. Gérard, I. Abram, L. Manin, and V. Thierry-Mieg, *Appl. Phys. Lett.* **79**, 2865 (2001).

⁷H. Pettersson, L. Bååth, N. Carlsson, W. Seifert, and L. Samuelson, *Appl. Phys. Lett.* **79**, 78 (2001).

⁸H. Pettersson, L. Bååth, N. Carlsson, W. Seifert, and L. Samuelson, *Phys. Rev. B* **65**, 073304 (2002).

⁹A. Schwarz, W. Allers, U. D. Schwarz, and R. Wiesendanger, *Appl. Surf. Sci.* **140**, 293 (1999).

¹⁰A. Schwarz, W. Allers, U. D. Schwarz, and R. Wiesendanger, *Phys. Rev. B* **61**, 2837 (2000).

¹¹A. Schwarz, W. Allers, U. D. Schwarz, and R. Wiesendanger, *Phys. Rev. B* **62**, 13617 (2000).

¹²F. J. Giessibl, *Science* **267**, 68 (1995).

¹³Y. Sugawara, M. Otha, H. Ueyama, and S. Morita, *Science* **270**, 1646 (1995).

¹⁴G. Binnig, C. F. Quate, and C. Gerber, *Phys. Rev. Lett.* **56**, 930 (1986).

¹⁵T. R. Albrecht, P. Grütter, D. Horne, and D. Rugar, *J. Appl. Phys.* **69**, 668 (1991).

¹⁶D. Drakova, *Rep. Prog. Phys.* **64**, 205 (2001).

¹⁷S. Morita, R. Wiesendanger, and E. Meyer, *Noncontact Atomic Force Microscopy* (Springer, Berlin, 2002).

¹⁸R. García and R. Pérez, *Surf. Sci. Rep.* **47**, 197 (2002).

¹⁹R. Pérez, M. C. Payne, I. Štich, and K. Terakura, *Phys. Rev. Lett.* **78**, 678 (1997).

²⁰R. Pérez, I. Štich, M. C. Payne, and K. Terakura, *Appl. Surf. Sci.* **140**, 320 (1999).

²¹I. Štich, J. Tóbiš, R. Pérez, K. Terakura, and S. H. Ke, *Prog. Surf. Sci.* **64**, 179 (2000).

²²H. Hölscher, W. Allers, U. D. Schwarz, A. Schwarz, and R. Wiesendanger, *Phys. Rev. B* **62**, 6967 (2000).

²³F. J. Giessibl, *Phys. Rev. B* **56**, 16010 (1997).

²⁴F. J. Giessibl and H. Bielefeldt, *Phys. Rev. B* **61**, 9968 (2000).

²⁵B. Gotsmann, C. Seidel, B. Ancykowski, and H. Fuchs, *Phys. Rev. B* **60**, 11051 (1999).

²⁶U. Dürig, *Appl. Phys. Lett.* **75**, 433 (1999).

²⁷K. J. Caspersen and J. W. Evans, *Phys. Rev. B* **64**, 075401 (2001).

²⁸H. Hölscher, W. Allers, U. D. Schwarz, A. Schwarz, and R. Wiesendanger, *Appl. Phys. A: Mater. Sci. Process.* **75**, S35 (2001).

²⁹W. Kohn and L. J. Sham, *Phys. Rev.* **140**, 1133 (1965).

³⁰S. H. Vosko, L. Wilk, and M. Nusair, *Can. J. Phys.* **58**, 1200 (1980).

³¹M. C. Payne, M. P. Teter, D. C. Allan, T. A. Arias, and J. D. Joannopoulos, *Rev. Mod. Phys.* **64**, 1045 (1992).

³²R. Berger, S. Blügel, A. Antons, W. Kromen, and K. Schroeder, in *Molecular Dynamics on Parallel Computers, Workshop am John von Neumann Institut für Computing, Jülich, 08–10. Feb. 1999*, edited by R. Esser, P. Grassberger, J. Grotendorst, and M. Lewerenz (World Scientific, Singapore, 2000), pp. 185–198.

³³B. Engels, P. Richard, K. Schroeder, S. Blügel, P. Ebert, and K. Urban, *Phys. Rev. B* **58**, 7799 (1998).

³⁴“Semiconductors: technology of III-V, II-VI and non-tetrahedrally bounded compounds,” *Landolt-Börnstein: Numerical Data and Functional Relationships in Science and Technology (New Series), Group III: Crystal and Solid State Physics* (Springer-Verlag, Berlin, 1984), Vol. 17d, Chap. 6.3, p. 13.

³⁵N. Sasaki, H. Aizawa, and M. Tsukada, *Appl. Surf. Sci.* **157**, 367 (2000).

³⁶S. H. Ke, T. Uda, and K. Terakura, *Phys. Rev. B* **65**, 125417 (2002).

³⁷M. Huang, M. Čuma, and F. Liu, *Phys. Rev. Lett.* **90**, 256101 (2003).

³⁸R. Pérez, I. Štich, M. C. Payne, and K. Terakura, *Phys. Rev. B* **58**, 10835 (1998).

³⁹S. H. Ke, T. Uda, R. Pérez, I. Štich, and K. Terakura, *Phys. Rev. B* **60**, 11631 (1999).

- ⁴⁰J. Tóbiš, I. Štich, and K. Terakura, Phys. Rev. B **63**, 245324 (2001).
- ⁴¹J. L. A. Alves, J. Hebenstreit, and M. Scheffler, Phys. Rev. B **44**, 6188 (1991).
- ⁴²H. J. Monkhorst and J. D. Pack, Phys. Rev. B **13**, 5188 (1976).
- ⁴³R. Bennowitz, A. S. Foster, L. N. Kantorovich, M. Bammerlin, C. Loppacher, S. Schär, M. Guggisberg, E. Meyer, and A. L. Shluger, Phys. Rev. B **62**, 2074 (2000).
- ⁴⁴A. S. Foster, C. Barth, A. L. Shluger, and M. Reichling, Phys. Rev. Lett. **86**, 2373 (2001).
- ⁴⁵C. Argento and R. H. French, J. Appl. Phys. **80**, 6081 (1996).
- ⁴⁶A. Schwarz (private communication).
- ⁴⁷J. Tóbiš, I. Štich, R. Pérez, and K. Terakura, Phys. Rev. B **60**, 11639 (1999).
- ⁴⁸S. H. Ke, T. Uda, I. Štich, and K. Terakura, Phys. Rev. B **63**, 245323 (2001).
- ⁴⁹S. M. Langkat, H. Hölscher, A. Schwarz, and R. Wiesendanger, Surf. Sci. **527**, 12 (2003).
- ⁵⁰A. Schwarz, Ph.D. thesis, University of Hamburg, 1998.